Surface-bonding geometry of (2×1)S/Ge(001) by the normal-emission angle-resolved photoemission extended-fine-structure technique

K. T. Leung,* L. J. Terminello, Z. Hussain,† X. S. Zhang,‡ T. Hayashi,§ and D. A. Shirley
Materials and Chemical Sciences Division, Lawrence Berkeley Laboratory, Berkeley, California 94720 and Department of Chemistry, University of California, Berkeley, California 94720
(Received 7 March 1988)

The surface structure of (2×1)S/Ge(001) was determined using the angle-resolved photoemission extended-fine-structure technique in the normal-emission direction. By comparison of the experimental data with curved-wave, multiple-scattering calculations, quantitative information about the local adsorption geometry was obtained. In particular, adsorption in a twofold bridge site, with a S—Ge bond length of 2.36 ± 0.05 Å, was found. The twofold S bridge appears most likely to occur between two partially intact symmetric Ge—Ge dimers, with the Ge dimer laterally displaced by 0.10 ± 0.05 Å from the bulk position. This result therefore provides evidence for S bonding to strong dangling bonds in the original dimers of the clean Ge(001) surface. There is, however, no evidence of significant surface contraction or expansion in the substrate layers, in contrast to the (2×2)S/Ge(111) case.

I. INTRODUCTION

Recent advances in the study of the photoelectron diffraction effect[1–4] using synchrotron radiation have demonstrated its effectiveness in accurate surface-structural determinations. In particular, measurements of the angle-resolved photoemission extended-fine-structure (ARPEFS) technique,[5,6] coupled with a combination of Fourier analysis[7] and a recently developed curved-wave, multiple-scattering theory,[8] have provided accurate determinations of the local surface-bonding geometry including adsorption sites, bond lengths, and bond angles. Detailed surface-structural information has been obtained for sulfur adsorbed on several metallic surfaces: Ni(001),[9] Ni(011),[10] Cu(001),[11] Mo(001),[12] and more recently on a semiconductor surface, Ge(111).[13] These studies have firmly established the methodology of the ARPEFS technique as well as providing new insights into our understanding of chemisorption in these systems.

The ARPEFS method is based on measuring the photoionization cross section of an adsorbate level over an extended range of photon energy (typically 500 eV), at appropriately chosen detection angles. The oscillatory modulations in the cross section (the extended fine structure) are caused by interference between direct propagation of a photoelectron wave and indirect trajectories of the photoelectron wave resulting from elastic scattering of neighboring ion cores. This fine structure therefore contains geometrical information about the surface. Extraction of the surface-geometrical information may involve direct Fourier analysis—generally applied as a qualitative investigation of the adsorption site—and a more quantitative R-factor analysis based on fitting the data with a curved-wave, multiple-scattering theory.[9] The ARPEFS technique is particularly suited for surface-structural determinations because of its chemical specificity, high surface and directional sensitivity, and large amplitude in the experimentally observed oscillations (typically ±20–50%). Furthermore, only a comparatively simple theoretical analysis [in contrast to low-energy-electron diffraction (LEED)] is required to extract geometrical information with high accuracy. To date, complete determinations of local surface structures have been achieved with accuracies of 0.02–0.05 Å.[9–12]

The surface structures of the (001) and (111) surfaces of Ge (and Si) represent prototype systems for investigation of surface-bonding phenomena involving double and single dangling bonds, respectively. These dangling bonds provide unique and interesting directional bonding possibilities on semiconductor surfaces that are not available in metallic systems. The surface electronic structure and reconstruction of clean Ge(001) have been studied by both low-energy-electron diffraction (LEED)[14,15] and angle-resolved photoemission.[16–20] However, relatively little work has been done on chemisorption of the Ge(001) surface. The existing adsorption studies include electron-energy-loss and infrared studies of hydrogen,[21–23] angle-resolved photoemission studies of Ag,[24] and other kinetic and thermal desorption studies of oxygen and alkali metals.[25] None of these methods are capable of providing quantitative information about the surface structure of these adsorbates on Ge(001). A recent photoemission study of S/Ge(001) (Ref. 26) suggests that sulfur is adsorbed in the bridge site. Another valence-band photoemission study of As/Si(001) shows that a symmetric As—As dimer is formed between two Si—As—Si bridges and further suggests that such a system can be used as a model for investigating dimerization of the dangling bonds and other surface reconstruction phenomena.[27] However, the nature of chemisorption involving these surface dangling bonds on Ge(001) [and Si(001)] is still largely unexplored. In an earlier work, we applied the ARPEFS technique to investigate the adsorbate structure of (2×2)S on Ge(111).[13] We now extend this work to study (2×1)S on Ge(001) using the ARPEFS method. These two systems should allow a comprehensive look at the bonding phenomena involving these dangling bonds and possibly provide some understanding of surface reconstruction.

II. EXPERIMENTAL

The ARPEFS measurements were performed on Beamline III-3 ("JUMBO") at the Stanford Synchrotron Radiation Laboratory using an angle-resolved multichannel photoelectron spectrometer.[28] Monochromatized photons in the range 2500–3000 eV were available from a double-crystal monochromator,[29] with a typical resolution of ≈ 2 eV full width at half maximum (FWHM). The light was over 98% linearly polarized. The angle-resolved multichannel photoelectron spectrometer was housed in an uhv chamber (base pressure $\approx 2\times10^{-10}$ Torr) equipped with LEED and retarding-field Auger electron spectroscopy (AES) capability. The spectrometer was operated at a constant pass energy of 160 eV during the experiment, giving an overall (monochromator plus spectrometer) energy resolution of ≈ 2.5 eV FWHM. The angular resolution of the spectrometer was typically 3° half-angle.

An ultrahigh-purity (undoped) Ge single crystal was cut and polished to within 1° of the (001) plane. It was chemically etched in a solution of 100-ml Mirrolux (Cabot Corp. Tuscola, Il) and 25 ml 30% H_2O_2. A clean Ge(001) surface was obtained after repeated cycles of Ar-ion sputtering at 500 eV and annealing to 550 °C. The clean surface was characterized by a strong (2×1) LEED pattern with two perpendicular domains of equal intensity. No contaminant was detectable by Auger measurements, using LEED optics operating in the retarding field mode.

Sulfur overlayers were obtained by exposure of the clean surface to H_2S gas (Matheson, 99.99% purity, used without further purification). A saturated coverage, as monitored by the ratio of S (152 eV) to Ge (89 eV) Auger intensities, was obtained after three to four cycles of exposures of ≈ 60 L (1 L $=1\times10^{-6}$ Torr sec), each followed by a 5-min anneal at 350 °C. At this coverage, the original double-domain (2×1) LEED pattern became slightly diffuse, with a general increase in the background. The persistance of the double-domain (2×1) LEED patterns from clean surface to sulfur-covered surface was also reported by Olshanetsky, Repinsky, and Shklyaer[30] for germanium-germanium sulphide systems. No degradation of the LEED pattern was observed over the course of the experiment, which typically lasted 12–20 h.

As noted by Weser *et al.* in their study of S/Ge(001),[26] sample preparation using H_2S may lead to coadsorption of H, HS, and S. In a separate chamber, we have studied the adsorption of H_2S on Ge(001) using high-resolution electron-energy-loss spectroscopy (EELS). Figure 1 shows the vibrational EEL spectra of a H_2S covered (50 L) Ge(001) surface after a series of 5-min anneals at different temperatures. These spectra were obtained in the specular direction with an incident energy of 1.6 eV and an incident angle of 50°, using a modified EEL spectrometer described elsewhere.[31] Typical energy resolution of this spectrometer was 5-meV FWHM. The spectrum of the unannealed sample [Fig. 1(a)] clearly shows the presence of two features: 244 meV corresponding to Ge-H stretch and 314 meV corresponding to S-H stretch. The vibrational modes for H_2S/Ge(001) were identified by comparison with gas-phase data.[32] The Ge-H stretching frequency observed in this work agrees with that of Papagno *et al.*[22] After a 5-min anneal at 200 °C, the S-H stretch was nearly gone, indicating the breakdown of H_2S and/or HS species [Fig. 1(b)]. At this point, the possible surface species were H and S. Further annealing to 300 °C for 5 min resulted in the disappearance of the Ge-H vibration, leaving S alone as the remaining adsorbate [Fig. 1(c)]. Although the Ge-S stretch which typically occurs at ≈ 70 meV for gas-phase complexes was obscured by the broad elastic peak (the peak width is believed to be related to the surface resistivity), the presence of S was identified by AES. By monitoring the Auger signals, it was further found that S started to desorb at ≈ 370 °C. The annealing temperature of 350 °C used in the ARPEFS experiments was based upon the EELS study. The identical sample holder and manipulator setup, as well as the sample heating procedure, were used in the two experiments. Annealing was achieved using electron bombardment from the back of a Ta sample plate, on which the crystal was mounted. The sample temperature was measured using a Chromel-Alumel thermocouple spot-welded at ≈ 1 cm above the crystal on the Ta plate. It was calibrated using an infrared pyrometer. This procedure was believed to yield an absolute accuracy of ≈ 50 °C. We therefore conclude that the ARPEFS sample was a S overlayer on the Ge(001) surface, without any other coadsorbates. The discrepancy in LEED patterns between Weser *et al.*[26] and the present work can be attributed to the differences in sample preparation.

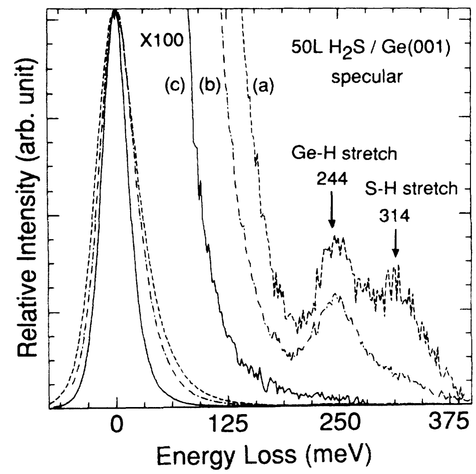

FIG. 1. Electron-energy-loss spectra of 50 L H_2S on Ge(001) taken in the specular direction with an incident energy of 1.6 eV and an incident angle of 50°. The (a) room-temperature sample was annealed at (b) 200 °C and (c) 300 °C for 5 min. The broad elastic peak is due to the surface resistivity of the undoped sample. The instrumental resolution of this spectrometer for a clean metal surface is 5 meV FWHM.

The ARPEFS experiment consisted of measuring a series of S (1s) core-shell kinetic-energy spectra (with a 20-eV wide window centered on the photopeak) for photon energies from $\approx$2500 to 3000 eV. The S (1s) peak areas were then extracted from individual spectra using a curve-fitting procedure described in detail elsewhere.[9,12] These areas were normalized using background curves measured typically 10 eV above the photopeak at several selected fixed photon energies, and converted to the experimental partial cross section after correction for the transmission function of the spectrometer. The extended fine structure $\chi(E)$ $[=I(E)/I_0(E)-1]$ was then extracted from the normalized partial cross section $I(E)$ by removing an arbitrary smooth atomiclike contribution $I_0(E)$. Details of the data reduction procedure can be found in Ref. 9. In the present work, ARPEFS curves of two samples were measured in the normal emission [001] direction, with the sample aligned such that the polarization vector of the incident photon beam was 35° to the surface normal and parallel to the [011] direction. The azimuthal direction of the crystal (with respect to the polarization vector) was chosen such that contributions to the ARPEFS intensity from the two domains [i.e., (1×2) and (2×1)] were equivalent. The alignment was achieved using laser autocollimation to an accuracy better than 2°.

III. RESULTS

Surface-structure determinations using the measured $\chi(E)$ curves can in general be separated into two steps: (1) determination of the adsorption site from all the possible sites and (2) quantitative determination of the surface bonding geometry using a R-factor minimization approach similar to LEED.[9] The absorption site can usually be determined through a qualitative evaluation of the possible path-length differences obtained from the Fourier transforms of the experimental χ curves measured in appropriately chosen detection directions. In the following, we will use the R-factor analysis for both adsorption-site and surface-geometry determinations, with the Fourier spectra being used only to illustrate and confirm the sensitivity of the theoretical results. The R-factor between the Fourier-filtered experimental curve, χ_{expt}, and the calculated curves χ_{theory} of a model structure using a curved-wave, multiple-scattering theory[8] is defined as before,[13] i.e.,

$$R=\int|\chi_{\text{expt}}(E)-\chi_{\text{theory}}(E)|^2dE \Big/ \int|\chi_{\text{expt}}(E)|^2dE\ .$$

The integrals were evaluated in the energy range from $\approx$77 to 420 eV, corresponding to a momentum range from 4.5 to 10.5 Å^{-1}.

The curved-wave, multiple-scattering (CWMS) theory[8] has been successful in accurate simulation of the experimental ARPEFS curves of all the systems studied to date. Detailed structural information can be obtained by minimization of the R factor calculated from the experimental curve and CWMS calculations of specific models of the surface geometry. The present analysis follows closely the work of Robey *et al.*[13] and employs similar values for the scattering parameters relevant in the CWMS calculations. In particular, similar values were used for the damping factor of the finite mean free path, and bulk and surface Debye temperatures. The phase shifts used for S and Ge for the present calculation were also identical to those in our earlier work,[13] where a detailed discussion of the phase-shift calculations was presented. The inner potential was set to be 10 eV, a value similar to the earlier work.[13] As before, a small variation in the inner potential does not change the general conclusions derived form the R-factor analysis.

Figure 2 shows the experimental $\chi(E)$ curves of two different samples, measured in the normal emission direction. The amplitudes of the observed oscillations for this system are rather small ($\pm10\%$ at best) and represent the smallest oscillations observed by the ARPEFS method to date. There is good reproducibility for the stronger features up to 250 eV, while the features in the higher kinetic-energy region lie within the experimental noise level (typically $\pm3\%$). The heavy solid line in the average curve [Fig. 2(c)] represents Fourier filtered data with filtering cutoffs at 1.0 and 11.5 Å^{-1}. Filtering was applied primarily to further reduce the low- and high-frequency noise arising from systematic effects such as possible photon beam movements, etc.[13] For consistency, a similar Fourier filtering procedure was also applied to the calculated curves before the R-factor analysis.

A. Determination of the adsorption site

In Fig. 3, we illustrate four possible unreconstructed sulfur adsorption sites on the Ge(001) surface. These include two bridge sites, an atop site and a four-fold site. It should be noted that two nonequivalent bridge sites are possible with the bridge-I site directly above a fourth-layer Ge atom and the bridge-II site directly above a

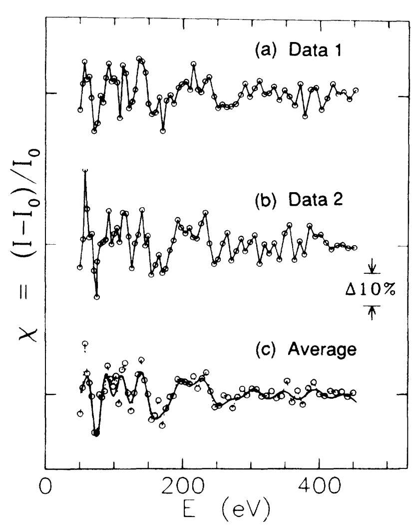

FIG. 2. Normal emission experimental χ curves as a function of the photoelectron kinetic energy E. The average of the two sets of data [(a) and (b)] is shown in (c). The solid line in (c) represents Fourier filtered data with filtering cutoffs at 4.5 Å^{-1} ($\approx$77 eV) and 10.5 Å^{-1} ($\approx$420 eV). The dashed line in (c) and the solid lines in (a) and (b) simply connect the data.

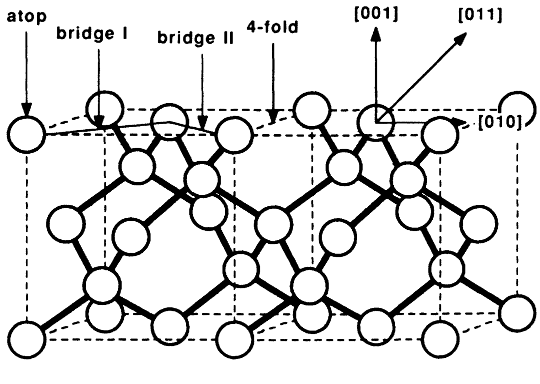

FIG. 3. Possible unreconstructed adsorption sites for S on Ge(001). Two Ge unit cells are shown along with the crystal orientations. Note that the bridge-I site is directly above a fourth-layer Ge atom while the bridge-II site is directly above a second-layer Ge atom.

second-layer Ge atom. In other words, bridge I lies parallel to the dangling bond direction while bridge II is perpendicular to it. In effect, the bridge-I site represents a "substitutional" site where a S overlayer replaces the next Ge layer.

Figure 4 compares the experimental $\chi(E)$ curve with two sets of theoretical curves calculated with the CWMS theory assuming two different S—Ge(1) (S to the first-layer Ge) interlayer distances and the bulk value (1.415 Å) for all the Ge—Ge interlayer distances. The respective S—Ge(1) interlayer distances, as well as the S—Ge(nearest) (S to the nearest Ge) distances (shown in brackets), are indicated in the figure. The solid lines correspond to S—Ge(nearest) distances of $\approx$2.3 Å, which

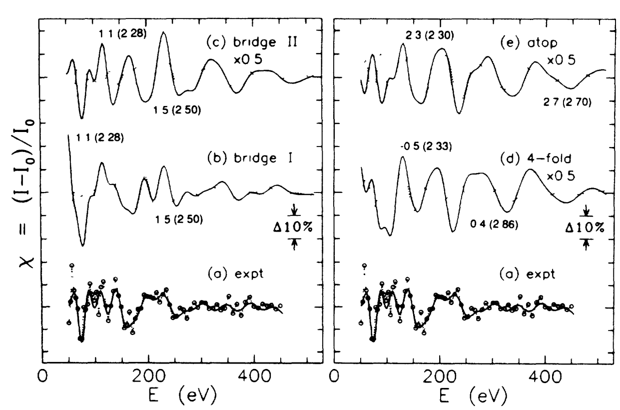

FIG. 4. Comparison of the experimental $\chi(E)$ curve with two sets of curved-wave, multiple-scattering calculations for the four possible adsorption sites. The bulk value (1.415 Å) is assumed for all the interlayer Ge—Ge distances. The S—Ge(1) (S to first layer Ge) interlayer distances (in Å), along with S—Ge(nearest) (S to the nearest Ge) distances (in Å and shown in brackets) are indicated. Note that the solid lines [in (b) to (e)] represent calculated curves assuming the most "probable" S—Ge(nearest) distance of $\approx$2.3 Å. Note also the scale change for (c), (d), and (e).

represents the Ge—S bond distance of the majority of Ge—S containing compounds. The dotted lines correspond to S—Ge(nearest) distances which give local minima in the R factor when the S—Ge(1) distance is varied (see Fig. 6). It is clear that the bridge-I site gives the best agreement with the experiment. All the other geometries give amplitudes generally too large by a factor of 2 as well as incorrect phases for the observed oscillations. It is also evident from a comparison between the two sets of CWMS calculations that varying the S—Ge(1) distance of the individual adsorption sites affects the calculated amplitudes and phases of the corresponding χ curves but does not change the above conclusion. The drastic changes in the ARPEFS curves corresponding to two different S—Ge(1) distances for the same adsorption geometry also demonstrate the sensitivity of the CWMS theory in modeling the surface structure.

This sensitivity is further illustrated in Fig. 5, which shows the Fourier transforms of the corresponding χ curves shown in Fig. 4. Only the bridge-I site gives a dominant Fourier peak at a path-length difference of $\approx$3.0 Å, in close agreement with the experimental data. Peaks in the Fourier spectra can be assigned to path-length differences associated with one or more particular scattering events. Considering only the solid curves, the dominant Fourier peak of each adsorption geometry, with the exception of the bridge-I site, corresponds to path-length differences arising from scattering of the S(1s) photoelectron wave from the Ge atom directly below the S atom. This demonstrates the fact that photoelectron diffraction is usually dominated by backward scattering events.[8] For the bridge-I site, the dominant Fourier peak corresponds to scattering off the bridging Ge atoms in the first Ge layer. In this geometry, backscattering from the fourth-layer Ge atom is weak due to the long path length. To summarize, the absence of a peak at $\approx$3 Å in the Fourier transform is strong evidence against the other three trial geometries.

Finally, we show in Fig. 6 the R factors for different

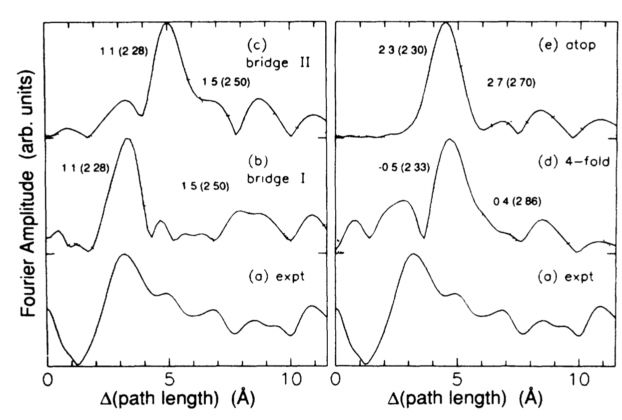

FIG. 5. Corresponding Fourier transforms of the χ curves shown in Fig. 4. The S—Ge(1) interlayer distances [and their corresponding S—Ge(nearest) distances] used for the calculations are indicated as in Fig. 4. Spectrum (a) corresponds to the Fourier spectrum of the unfiltered experimental data.

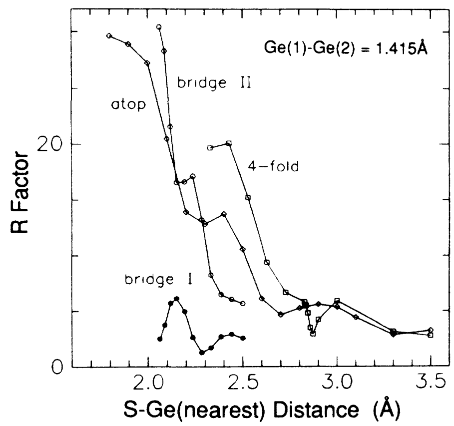

FIG. 6. R factor as a function of S-to-the-nearest-Ge distance for the four possible adsorption sites considered in Fig. 3. As before, the bulk value (1.415 Å) is used for all the Ge—Ge interlayer distances for the calculations. Only the S—Ge(1) distance was varied.

bonding sites as a function of S—Ge(nearest) distance obtained by varying the S—Ge(1) distance (with all the other Ge—Ge interlayer distances set at the bulk value). The S—Ge(1) distance used in the R-factor analysis for each adsorption site lie within the nominal limits for the Ge—S bond lengths found in most Ge—S containing compounds. It should be noted that the majority of known Ge—S bond lengths lies between 2.05 to 2.44 Å, with most lying in the range 2.15–2.20 Å.[13] It is clear that the bridge-I site gives the lowest R factor, with a parabolic minimum at 2.28 Å. The top site and the fourfold site give considerably larger R factors with local minima at 2.70 and 2.86 Å, respectively. Both are outside the expected limits of most Ge—S containing compounds.

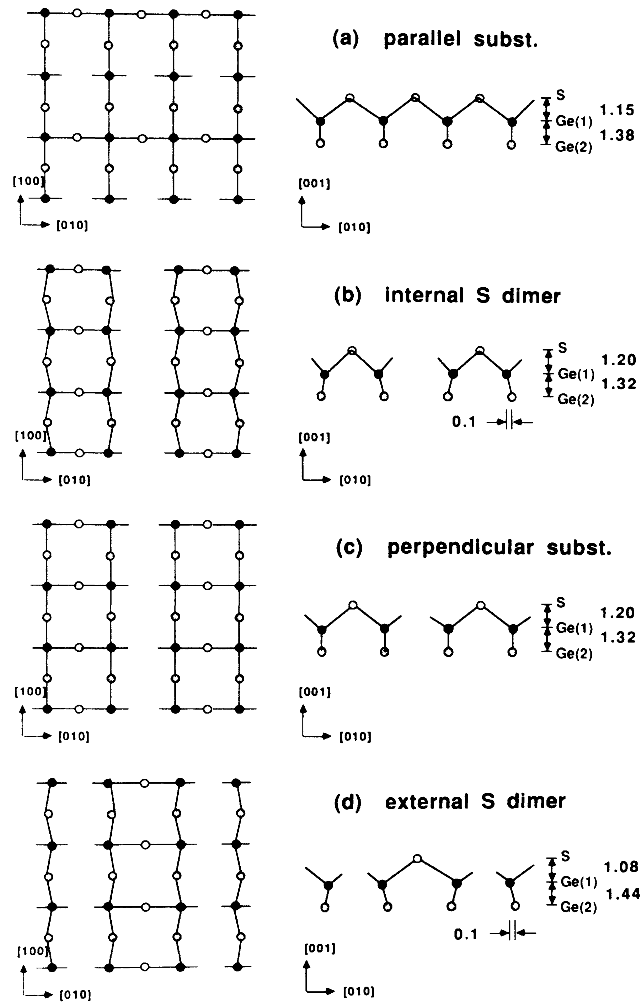

FIG. 7. Schematic models of surface structures for (2×1)S/Ge(001) compatible with the bridge-I site and the observed LEED pattern. Optimal interlayer distances as well as lateral displacements (in Å) for individual geometries are indicated in the side views. The bulk value (1.415 Å) is assumed for all other Ge—Ge interlayer (not shown) distances. Note that the figures are not drawn to scale.

B. Quantitative determination of the local surface geometry

Four simple (two unreconstructed and two reconstructed) bonding geometries, compatible with the bridge-I site and the observed double-domain (2×1) LEED pattern, are considered for the final structure determination. These bonding geometries are illustrated in Fig. 7. For the unreconstructed substitutional sites, two different arrangements are compatible with the (2×1) long-range order, depending upon whether S-S nearest-neighbor direction is parallel [parallel substitutional, Fig. 7(a)] or perpendicular [perpendicular substitutional, Fig. 7(c)] to the dangling bond direction. For the unreconstructed symmetric dimer sites, the S atom can be placed inside the symmetric Ge—Ge dimer [internal S, Fig. 7(b)] or between two Ge—Ge symmetric dimers [external S, Fig. 7(d)]. Assuming the bulk value for all interlayer distances for Ge, we performed a R-factor minimization search for the optimal geometry by varying the S—Ge(1) distance and the Ge(1)—Ge(2) interlayer distance. In the case of the symmetric dimers, such a minimization search was also performed as a function of the lateral displacement from the bulk position (i.e., from the perpendicular substitutional site). A lateral displacement of 0.10 Å was found to be optimal in both cases.

The CWMS theoretical χ curves which give the lowest R factors for each of the corresponding bonding geometries are compared with the experiment in Fig. 8. (The bonding parameters of the respective geometries are shown in Fig. 7). It is clear that none of the calculated curves simulates experiment satisfactorily below ≈ 100 eV, where we observe, as in the (2×2)S/Ge(111) case,[13] that the CWMS theory performs poorly.[8] In the higher energy regime, the external-S symmetric dimer appears to give better overall agreement with experiment. We shall base our further discussion on this geometry, although the other three geometries are not ruled out, given the similarity of the curves in Fig. 8 and the experimental error.

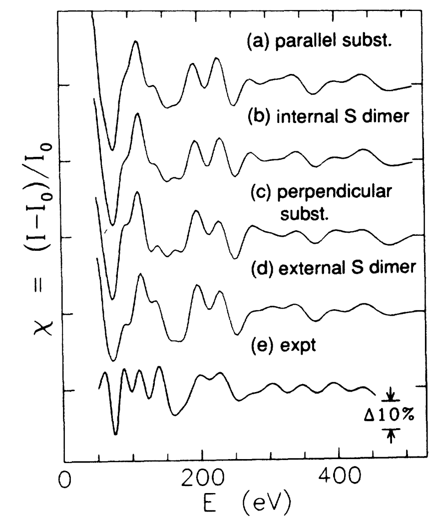

FIG. 8. Comparison of the filtered experimental $\chi(E)$ curve to the curved wave, multiple scattering calculations for the four bridge-I surface structures considered in Fig. 7. The calculated curves were generated using the optimal interlayer distances (as indicated in Fig. 7) in the respective surface structures.

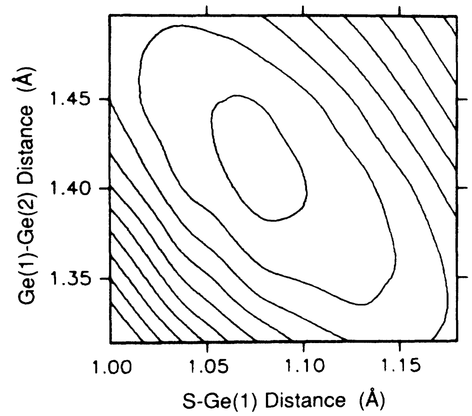

FIG. 10. Contour plot of the R factor for the external S dimer case. The S—Ge(1) and Ge(1)—Ge(2) interlayer distances corresponding to the R-factor minimum are 1.08 and 1.41 Å, respectively. Note that a Ge(2)—Ge(3) interlayer distance of 1.455 Å was used for the calculation, with all the other Ge—Ge interlayer distances set at the bulk value (1.415 Å)

Finally, assuming the external-S symmetric dimer bonding geometry, R-factor minimization as a function of S—Ge(1) and Ge(1)—Ge(2) distances was performed for different Ge(2)—Ge(3) interlayer distances. These CWMS calculated curves, corresponding to the minima of the R-factor maps for individual Ge(2)—Ge(3) distances, are compared with experiment in Fig. 9. A Ge(2)—Ge(3) distance of 1.46 Å was found to give the lowest R factor. The R-factor contour map corresponding to this optimal external-S symmetric dimer geometry is shown in Fig. 10, from which we derive the optimal S—Ge(1) and Ge(1)—Ge(2) interlayer distances to be 1.08 and 1.41 Å, respectively.

In summary, the sulfur atom is adsorbed in a bridge-I site on a Ge(001) surface. The Ge—S—Ge bridge may connect two partially intact Ge—Ge symmetric dimers, although other variants give very similar theoretical curves. Specific local surface-structural parameters obtained by using the R-factor analysis with CWMS simulations are given in Fig. 11. Of these four parameters, the 0.1-Å lateral displacement of S has only weak support—it is the symmetric-dimer option. The other parameters are not very sensitive to this choice.

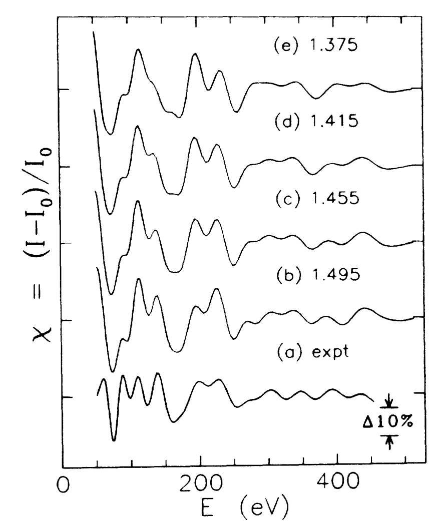

FIG. 9. Comparison of the filtered experimental $\chi(E)$ curve to the curved wave, multiple scattering calculations assuming the external S dimer model and several values of the interlayer distances (in Å) between the second and third Ge layers.

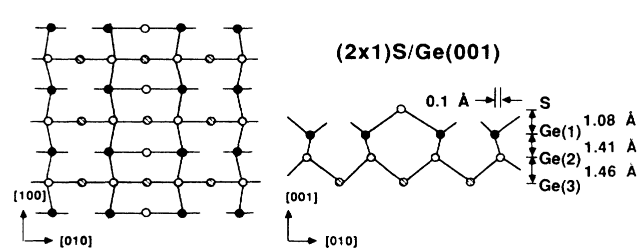

FIG. 11. The surface bonding geometry of (2×1)S/Ge(001) determined by the ARPEFS method. Note that the result does not give information about the planarity of the Ge layers. Therefore only interlayer distances and the lateral displacement from the bulk position are indicated and are rounded off to the nearest 0.01 Å.

IV. DISCUSSION

We have determined the surface structure of (2×1)S/Ge(001) by fitting the experimental S(1*s*) core-shell photoemission extended fine structure measured in the normal emission direction to CWMS calculations.[9] The S/Ge(001) system has critically tested the present treatment of structural determination because of its rather small oscillations. Based upon the sensitivity of the CWMS theory in distinguishing different adsorption sites, the *R*-factor minimization procedure remains valid and essential in the present analysis. The accuracies in the derived structural parameters therefore depend on the quality of the measured data. For metallic systems such as S/Ni(001) where ±50% oscillations were found,[9] a noise level of ±3% (typical in most ARPEFS measurements) in the χ curves gave a signal-to-noise ratio of 17. To achieve the same signal-to-noise ratio in the present case where typical oscillations are ±10% at best, the allowed noise level in the measured χ curves would have to be reduced to ±0.6%. It is difficult to achieve this kind of data quality given the constraints of the available beam time at present-day synchrotron radiation facilities. As a result, even though the derived Ge(2)—Ge(3) distance (1.46 Å) is greater than the bulk value (1.415 Å), the experimental uncertainty does not allow a definitive conclusion to be made about surface expansion. Within the experimental errors, we may only conclude that there is little evidence for surface contraction or expansion for (2×1)S/Ge(001). The derived Ge(1)—Ge(2) distance is essentially the bulk value. Sulphur adsorption therefore appears to suppress the original surface reconstruction of the clean Ge(001) surface proposed in the LEED analysis.[14]

There are some similarities in the bonding geometries between the (2×2)S/Ge(111) case[13] and the present (2×1)S/Ge(001) case. In particular, both the two-fold bridge adsorption site and an identical Ge—S—Ge bond angle (i.e., 125°) are found in the two cases. The two-fold bridge site was also suggested for S/Ge(001) in a recent photoemission study by Weser *et al.*[26] It was also found to be the most stable site for O adsorption on Si(001) and Si(111) surfaces in a recent MNDO cluster theoretical study.[33] The present bonding geometry, however, gives a considerably larger bond length [2.36(5) Å] when compared with the Ge(111) case [2.23(5) Å] and with the sum of the covalent bond radii of S and Ge (2.26 Å).

The derived geometry is consistent with the idea that dimerization of the dangling bonds exists on the clean surface. The S atom consumes the remaining dangling bond of a Ge atom by forming a bridge between two Ge—Ge dimers. The somewhat long bond length observed in the present experiment further suggests that the original Ge—Ge dimer bond is rather strong and that the formation of the S bridge only suppresses the (2×1) reconstruction. Previous LEED studies[14,15] of the structure of clean Ge(001) surface proposed several models to explain the observed (2×1) reconstruction. These include the missing row, the symmetric and asymmetric dimers and the conjugate chain models, with the latter being most popular.[14] The dimer models considered in the LEED calculations give typical lateral displacements of 0.72 Å for symmetric dimers and 0.46–1.13 Å for asymmetric dimers.[14] The present work gives a lateral displacement of only 0.10 Å, considerably smaller than a "true" symmetric dimer case. A recent infrared study of hydrogen adsorption on Si(001) and Ge(001) (Ref. 23) reported the formation of only monohydride on a H-saturated Ge(001) surface, in contrast to the hydrogen on Si(001) case where both monohydride and dihydride were observed. This study further suggested that the Ge—Ge dimer was more stable than the Si—Si dimer. Furthermore, a recent photoemission study of Ag/Ge(001) by Miller, Rosenwinkel, and Chiang[24] also inferred weak bonding between the adsorbate and the surface and suggested the suppression of (2×1) reconstruction of Ge(001) due to Ag adsorption. All of these studies together confirm that the Ge—Ge dimer bond is strong and that adsorption of H,[23] Ag,[24] and in the present case S only suppresses the (2×1) reconstruction.

Other bonding variations of the bridge-I site incorporating the more popular models such as the asymmetric dimer and the conjugate chain models for the Ge(001) surface were also considered in the ARPEFS simulation. None produce a lower *R* factor than that of the external-S symmetric dimer model. We emphasize, however, that the surface structure determined for the S covered Ge(001) surface in the present work (or indeed any adsorbate study) would not determine which dimer model is correct for the clean Ge(001) surface because adsorption of S may symmetrize the Ge—Ge dimer and significantly alter the original reconstruction of the clean surface. The present result only provides additional evidence, not proof, for the existence of the Ge—Ge dimer bond.

The present work is also consistent with the recent photoemission study of As/Si(001) by Uhrberg *et al.*[27] In this work, the surface structure was determined by comparison of a pseudopotential calculation to the observed band structure. It was found that a model consisting of a symmetric As—As dimer of two Si—As—Si bridges gave the best agreement with experiment. The key feature is that the trivalent As atom satisfies all of its available valencies by forming the As—As dimer, in addition to the Si—As—Si bridge formation. For a divalent adsorbate such as S, such an additional dimerization is not necessary. We may therefore conclude that, like the As on Si case, simple valence bond theory appears to work for S adsorption on Ge(001) and Ge(111) surfaces. Finally, it is interesting to note that the bond length for the Si—As back bond (2.44 Å) was also found to be larger than the sum of the covalent radii of the individual bonding partners (2.33 Å), as is also found in the present work.

ACKNOWLEDGMENTS

This work was supported by the Director, Office of Energy Research, Office of Basic Energy Sciences, Chemical

Sciences Division of the U.S. Department of Energy under Contract No. DE-AC03-76SF00098. It was performed at the Stanford Synchrotron Radiation Laboratory, which was supported by the Office of Basic Energy Sciences, Department of Energy. One of us (K.T.L.) gratefully acknowledges support from the Natural Sciences and Engineering Research Council of Canada and the Killam Foundation.

---

*Present address: Department of Chemistry, University of Waterloo, Waterloo, Ontario, Canada N2L 3G1.

†Permanent address: Department of Physics, University of Petroleum and Minerals, Dhahran, Saudi Arabia.

‡Permanent address: Department of Physics, Zhejiang University, Hongzhou, People's Republic of China.

§Permanent address: Material Evaluation Section, Nippon Telephone and Telegraph Electrical Communications Laboratories, Tokyo 180, Japan.

[1]A. Liebsch, Phys. Rev. Lett. **32**, 1203 (1974).

[2]S. D. Kevan, D. H. Rosenblatt, D. Denley, B. C. Lu, and D. A. Shirley, Phys. Rev. Lett. **41**, 1565 (1978).

[3]S. Kono, C. S. Fadley, N. F. T. Hall, and Z. Hussain, Phys. Rev. Lett. **41**, 117 (1978); S. Kono, S. M. Goldberg, N. F. T. Hall, and C. S. Fadley, *ibid.* **41**, 1831 (1978).

[4]D. P. Woodruff, D. Norman, B. W. Holland, N. V. Smith, H. H. Farrell, and M. M. Traum, Phys. Rev. Lett. **41**, 1130 (1978).

[5]J. J. Barton, C. C. Bahr, Z. Hussain, S. W. Robey, J. G. Tobin, L. E. Klebanoff, and D. A. Shirley, Phys. Rev. Lett. **51**, 272 (1983); J. J. Barton, C. C. Bahr, Z. Hussain, S. W. Robey, L. E. Klebanoff, and D. A. Shirley, J. Vac. Sci. Technol. A **2**, 847 (1986).

[6]J. J. Barton, Ph.D. thesis, University of California, Berkeley, 1985.

[7]Z. Hussain, D. A. Shirley, C. H. Li, and S. Y. Tong, Proc. Natl. Acad. Sci. (USA) **78**, 5293 (1981).

[8]J. J. Barton, S. W. Robey, and D. A. Shirley, Phys. Rev. B **34**, 778 (1986).

[9]J. J. Barton, C. C. Bahr, S. W. Robey, Z. Hussain, E. Umbach, and D. A. Shirley, Phys. Rev. B **34**, 3807 (1986).

[10]S. W. Robey, J. J. Barton, C. C. Bahr, G. Liu, and D. A. Shirley, Phys. Rev. B **35**, 1108 (1987).

[11]C. C. Bahr, J. J. Barton, Z. Hussain, S. W. Robey, J. G. Tobin, and D. A. Shirley, Phys. Rev. B **35**, 3773 (1987).

[12]C. C. Bahr, S. W. Robey, Z. Hussain, L. J. Terminello, K. T. Leung, J. R. Lou, A. E. Schach von Wittenau, and D. A. Shirley (unpublished).

[13]S. W. Robey, C. C. Bahr, Z. Hussain, J. J. Barton, K. T. Leung, J. R. Lou, A. E. von Wittenau, and D. A. Shirley, Phys. Rev. B **35**, 5657 (1987).

[14]J. C. Fernandez, W. S. Yang, H. D. Shih, F. Jona, D. W. Jepsen, and P. W. Marcus, J. Phys. C **14**, L55 (1981).

[15]F. Jona, H. D. Shih, D. W. Jepsen, and P. W. Marcus, J. Phys. C **12**, L455 (1979), and references therein.

[16]J. G. Nelson, W. J. Gignac, R. S. Williams, S. W. Robey, J. G. Tobin, and D. A. Shirley, Phys. Rev. B **27**, 3924 (1983).

[17]D. V. Froelich, M. A. Bowen, and J. D. Dow, J. Vac. Sci. Technol. B **2**, 390 (1984).

[18]S. D. Kevan and N. G. Stoffel, Phys. Rev. Lett. **53**, 702 (1984).

[19]T. C. Hsieh, T. Miller, and T. C. Chiang, Phys. Rev. B **30**, 7005 (1984).

[20]S. D. Kevan, Phys. Rev. B **32**, 2344 (1985).

[21]L. Surnev and M. Tikhov, Surf. Sci. **138**, 40 (1984).

[22]L. Papagno, X. Y. Shen, J. Anderson, G. Schirripa Spagnolo, and G. J. Lapeyre, Phys. Rev. B **34**, 7188 (1986).

[23]Y. J. Chabal, Surf. Sci. **168**, 594 (1986).

[24]T. Miller, E. Rosenwinkel, and T. C. Chiang, Solid State Commun. **50**, 327 (1984); Phys. Rev. B **30**, 570 (1984).

[25]L. Surnev and M. Tikhov, Surf. Sci. **123**, 505 (1982); **123**, 519 (1982); **118**, 267 (1982).

[26]T. Weser, A. Bogen, B. Konrad, R. D. Schnell, C. A. Schug, and W. Steinmann, Phys. Rev. B **35**, 8184 (1987).

[27]R. I. G. Uhrberg, R. D. Bringans, R. Z. Bachrach, and J. E. Northrup, Phys. Rev. Lett. **56**, 520 (1986). See also R. D. Bringans, R. I. G. Uhrberg, M. A. Olmstead, and R. Z. Bachrach, Phys. Rev. B **34**, 7447 (1986).

[28]S. D. Kevan, Ph.D. thesis, University of California, Berkeley, 1980.

[29]Z. Hussain, E. Umbach, D. A. Shirley, J. Stohr, and J. Feldhaus, Nucl. Instrum. Methods **195**, 115 (1982).

[30]B. Z. Olshanetsky, S. M. Repinsky, and A. A. Shklyaev, Surf. Sci. **64**, 224 (1977).

[31]M. A. Schultz, M.Sc. thesis, University of California, Berkeley, 1985, and references therein. See also K. T. Leung, X. S. Zhang, and D. A. Shirley (unpublished).

[32]See, for example, E. Maslowsky, Jr., *Vibrational Spectra of Organometallic Compounds* (Wiley, New York, 1977); Takehiko Shimanouchi, U.S. Department of Commerce, National Bureau of Standards Report No. NSRDS-NBS39, 1972 (unpublished).

[33]N. Russo, M. Toscano, V. Barone, and F. Lelj, Phys. Lett. **113A**, 321 (1985).